The Annual Final Scientific Report:

Toxicity and Bio-Safety Evaluation of Magnetic Nanocrystals Designed for Nano-Medical Sensors

Key researchers: Jinwoo Cheon

Affiliation: Department of Chemistry, Yonsei University

Address: 134 Shinchon-dong, Seodaemun-gu, Seoul 120-749, Korea

Tel: 82-2-2123-5631, fax: 82-2-364-7050, email: jcheon@yonsei.ac.kr

Table of Content

* Appendix: The first page and the page including acknowledgement part of the published papers.

Report Documentation Page

1. REPORT DATE	2. REPORT TYPE	3. DATES COVERED
15 SEP 2006	**FInal**	**23-02-2005 to 11-06-2006**

4. TITLE AND SUBTITLE	5a. CONTRACT NUMBER
Toxicity and Bio-safety Evaluation of Magnetic Nanocrystals Designed for Nano-medical Sensors	**FA520905P0285**
	5b. GRANT NUMBER
	5c. PROGRAM ELEMENT NUMBER

6. AUTHOR(S)	5d. PROJECT NUMBER
Jinwoo Cheon	5e. TASK NUMBER
	5f. WORK UNIT NUMBER

7. PERFORMING ORGANIZATION NAME(S) AND ADDRESS(ES)	8. PERFORMING ORGANIZATION REPORT NUMBER
Yonsei University,134 Shinchon-dong, Seodaemun-gu,Seoul 120-749,Korea (South),KR,120-749	**N/A**

9. SPONSORING/MONITORING AGENCY NAME(S) AND ADDRESS(ES)	10. SPONSOR/MONITOR'S ACRONYM(S)
AOARD, UNIT 45002, APO, AP, 96337-5002	**AOARD**
	11. SPONSOR/MONITOR'S REPORT NUMBER(S)
	AOARD-054048

12. DISTRIBUTION/AVAILABILITY STATEMENT
Approved for public release; distribution unlimited

13. SUPPLEMENTARY NOTES

14. ABSTRACT
Magnetic nanocrystals exhibit unique superparamagnetic behaviors. When they get into bio-medical systems, these magnetic nanocrystals have the potential to be utilized as probes and vectors for next-generation diagnosis and therapy. However, before one can utilize these nanomaterials in biology, it is important to assess if they have any deleterious properties in biological systems. In this project, toxicity and biosafety of magnetic nanocrystals under both in vitro and in vivo conditions are examined. In specific, cytotoxicity of inverse spinel metal ferrite nanocrystals with four different magnetic compositions (i.e. Fe_3O_4, $MnFe_2O_4$, $CoFe_2O_4$, $NiFe_2O_4$) on macrophage cells is investigated. Nanocrystal (Fe_3O_4) surface charge effect on cellular cytotoxicity are further examined. In addition to such in vitro cellular toxicity of nanocrystals, in vivo biodistribution of Fe_3O_4 nanocrystals are examined by labeling them with radio-active 111In-DTPA.

15. SUBJECT TERMS
Chemistry, Nanotechnology, Magnetic Resonance Spectroscopy

16. SECURITY CLASSIFICATION OF:			17. LIMITATION OF ABSTRACT	18. NUMBER OF PAGES	19a. NAME OF RESPONSIBLE PERSON
a. REPORT	b. ABSTRACT	c. THIS PAGE	**Same as Report (SAR)**	**22**	
unclassified	**unclassified**	**unclassified**			

1. Abstract

Magnetic nanocrystals exhibit unique superparamagnetic behaviors. When they get into bio-medical systems, these magnetic nanocrystals have the potential to be utilized as probes and vectors for next-generation diagnosis and therapy. However, before one can utilize these nanomaterials in biology, it is important to assess if they have any deleterious properties in biological systems. In this project, we examined toxicity and biosafety of magnetic nanocrystals under both *in vitro* and *in vivo* conditions. In specific, cytotoxicity of inverse spinel metal ferrite nanocrystals with four different magnetic compositions (i.e. Fe_3O_4, $MnFe_2O_4$, $CoFe_2O_4$, $NiFe_2O_4$) on macrophage cells was investigated. We further examined nanocrystal (Fe_3O_4) surface charge effect on cellular cytotoxicity. In addition to such in vitro cellular toxicity of nanocrystals, in vivo biodistribution of Fe_3O_4 nanocrystals were examined by labeling them with radio-active ^{111}In-DTPA.

Proposed Research
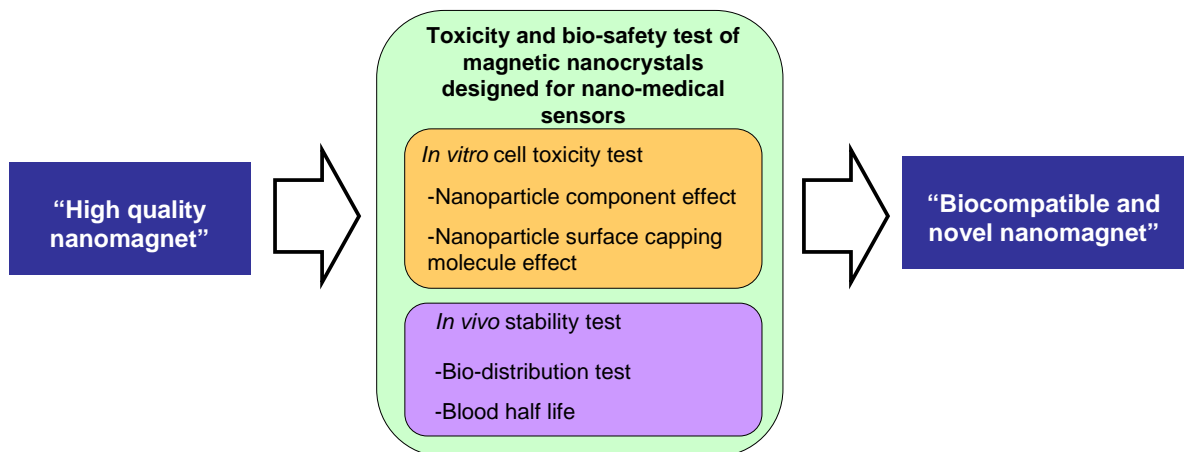
2. Introduction

Inorganic nanocrystals with unique quantum mechanical properties have the potential to revolutionize current classical mechanics-based science and industry. In particular, when these tiny materials get into biological system, their exceptionally enhanced properties can enable them to be utilized as key probes and vectors for next-generation ultra-sensitive detection and highly efficient therapeutic systems. During past few years, researches on this field have been explosively carried out and some of successful studies have shown such possibilities in part. However, before one can utilize these nanocrystals in clinical system, it is very important to examine their toxicity and bio-safety and to establish a guide for their proper use in biological system. The unique, novel and enhanced physical and chemical characteristic of nanocrystals differentiated with their counter part, bulk material, leads dramatic improvements for various field including biomedical, electric, device, and storage applications. Especially, in biomedical purpose, tunability of the nanocrystal line properties through controlling their size, shape, and composition make these materials useful and optimized. Combined with biomaterials, nanocrystals are widely used in biological sensing, detection, and therapeutic systems including fast immunoassay separation & detection of bio-molecules (e.g. cell or DNA.), ultra-sensitive MRI (magnetic resonance imaging) contrast agent for in vivo disease detection, and target specific drug delivery system.

In our previous study, we developed a nanotechnology-associated magnetic resonance imaging (nano-MRI) technique by utilizing magnetic nanocrystals with well-defined size, single crystallinity, and enhanced magnetic property. Utilization of these high quality nanomagnets as MR contrast agents provides highly sensitive detection of cancer under both *in vitro* and *in vivo* conditions. As a following study, in this project, we have further investigated their toxicity. In specific, we have focused on the the composition and surface property effects of magnetic nanocrystals on cytotoxicity to live cells and living subjects (i.e. mouse). This exploration will be very important for the development of nano-platform for biological system such a bio-compatible probe with high quality and excellent MR contrasting effect for MRI.
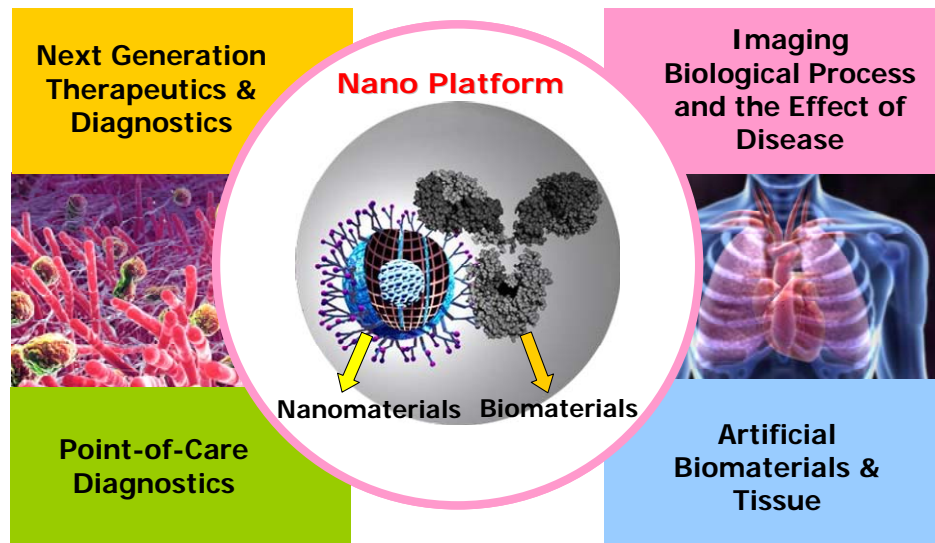
Fig 1. Nano Platform, the next generation nanosystem for biomedical purpose.

3. Approach

We *i*) first synthesized various magnetic nanocrystals through a high temperature molecular precursor decomposition method in a appropriate organic medium. With these nanocrystals synthesized, *ii*) elucidation of the nanocrystal toxicity depending on the nanocrystal composition was conducted. As a case study, we examined the composition effects of inverse spinel magnetic nanocrystals on *in vitro* toxicity to macrophage cells by systematically changing M as Mn, Fe, Co, and Ni. Then, *iii*) we further examined in vivo pharmacokinetic studies of 12 nm Fe_3O_4 nanocrystals in a living animal (mouse), which include bio-distribution and blood half life time of the nanocrystals.

3-1-1. Synthesis of magnetic nanocrystals

In this research, we synthesized various types of magnetic nanocrystals including inverse spinel metal ferrites (e.g. Fe_3O_4, $MnFe_2O_4$, $CoFe_2O_4$, & $NiFe_2O_4$), cobalt nanocrystals, and core-shell Co@Pt. We adopted a high temperature molecular precursor decomposition method in nonhydrolytic media which provides high quality single crystalline stoichiometric magnetic nanocrystals. As-synthesized nanocrystals were coated with hydrophobic ligands and therefore insoluble in water. In order to make them water soluble, hydrophilic ligands, 2,3-dimercaptocuccinic acid, were introduced onto the nanocrystal surface via appropriate ligand exchange procedures.

3-1-2. In vitro toxicity of metal ferrite nanocrystals

We first examined the in vitro cytotoxicity of various metal ferrite nanocrystals (e.g. Fe_3O_4, $MnFe_2O_4$, $CoFe_2O_4$, & $NiFe_2O_4$) on U937 macrophage cells. In specific, we focused on the core metal composition effect of nanocrystals, since this can significantly influence on their cytotoxicity on the cells when metal ions are leaching from the nanocrystals. As a comparison, cytotoxicity of free divalent metal ion compounds (i.e. $FeCl_2$, $MnCl_2$, $CoCl_2$, & $NiCl_2$) was also examined through identical procedures used in metal ferrite toxicity study. Cells were incubated in a culture medium containing appropriate amounts of each nanocrystal. After 2 days, cell viability was evaluated by either FITC-Annexin-V fluorescent activated cell sorting (FACS).

3-1-3. Biodistribution of metal ferrite nanocrystals

In vivo behaviors of metal ferrite nanocrystals were examined through bio-distribution study of them in a live mouse. The magnetic nanocrystal was first conjugated with the

radio active isotope, ^{111}In-DTPA, then intravenously injected into a nude mouse (n = 3). At 24 hrs, the mouse was sacrificed and dissected and samples of the tumor, liver, spleen, and muscle were taken. Radioactivity of each sample was measured by a γ-counter (COBRA Quantum 5015, Packard, USA). The percentage of the injected dose per gram (%ID/g) of tissue was calculated.

3-2. Uniqueness of approach

In the previous research grant (grant # N62649-03-2-0008), we developed magnetic nanocrystals with various sizes and shapes via both the molecular designed approach and the bio-mimetic approach. These nanocrystals are the key component for biological sensing, detection, and therapeutic systems including fast immunoassay separation & detection of bio-molecules (such as cell or DNA), ultra-sensitive MRI (magnetic resonance imaging) contrast agent for *in vivo* disease detection, and target specific drug delivery system.

Before utilizing them as nanoscale sensing elements for *in vitro* and *in vivo* clinical applications, it is very important to examine the toxicity and health effects of the nanocrystals onto the biological molecules and living systems (e.g. animal). In this project, we examine the toxicity and health effects of ultra-small (< 30 nm) bio-mimetic magnetic nanocrystals and optimize the biocompatibility of the magnetic nanocrystals by modifying the nanocrystal surface functionality (e.g. capping molecules) and the compositon.   From this study, development of well defined magnetic nanocrystals with high bio-compatibility and low toxicity is possible and this accelerates the creation of next generation nanosystems for unique applications of biomedical technology.

3-3 Research contents

The 1st stage: Synthesis of magnetic nanocrystals

- Fabrication of inverse spinel metal ferrite magnetic nanocrystals
- Synthesis of metallic Co and Co/Pt core/shell nanocrystals

The 2nd stage: Evaluation of *in vitro* cytotoxicity of metal ferrite nanocrystals

- Cytotoxicity of MFe_2O_4 nanocrystals (M = Fe, Mn, Co, Ni).

The 3rd stage: Biodistribution study of MFe_2O_4 nanocrystals

- Biodistribution of $MnFe_2O_4$ nanocrystals in a live nude mouse

4. Results and discussion

4-1. Synthesis of various magnetic nanocrystals

At the early stage of this project, we performed the synthesis of various magnetic nanocrystals through nonhydrolytic high temperature thermal reaction protocol. Metal precursors and surfactants are dissolved in organic solvents and heated to reflux. Then reaction solution was cooled to room temperature when the reaction finished. With the method we could synthesized various nanocrystals with high monodispersity and excellent crystallinity which lead remarkably enhanced magnetic property. As shown in figure 3, various nanocrystals were synthesized, including metal oxides, metal, and core shell type, with narrow size distribution (~10 %). (J. Cheon *et. al. J. Phys. Chem. B* **2005**, *109*, 13119.; *Chem. Commun.* **2006**, 1619.; *Angew. Chem.* **2006**, *45*, 3414.)
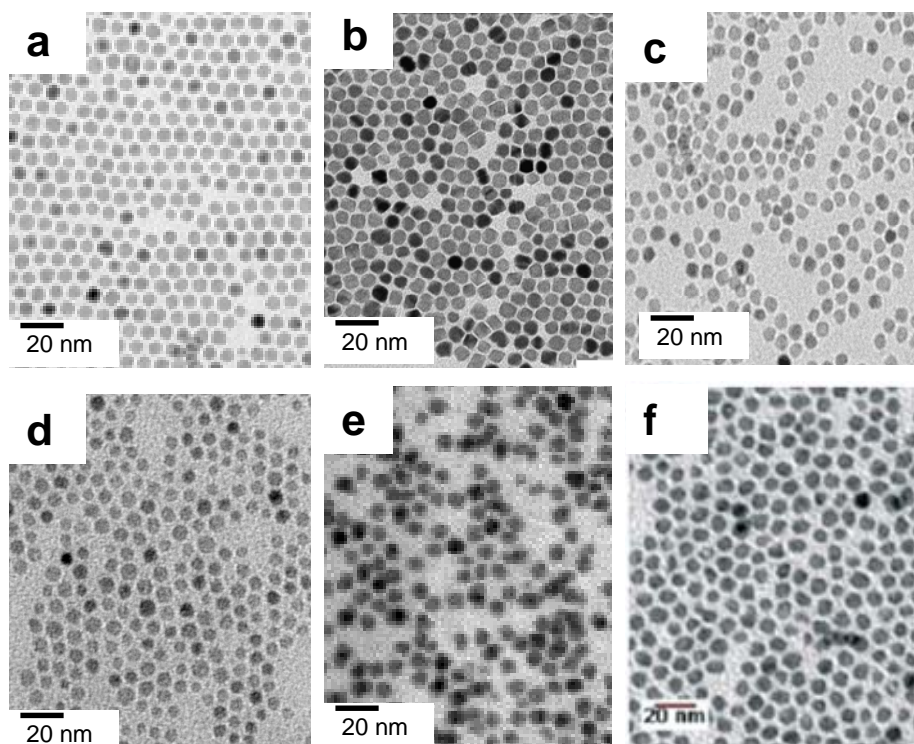
Fig 3. TEM images of various magnetic nanocrystals. (a) Fe_3O_4, (b) $MnFe_2O_4$, (c) $CoFe_2O_4$, (d) $NiFe_2O_4$, (e) $CoFe_2O_4$, and (f) Co@Pt.

4-2. Toxicity study of nanocrystals

According to our FACS analyses, all metal ferrite nanocrystals synthesized are biologically non-toxic in the tested nanocrystal concentration of 60 μg/ml. In contrast, only Fe^{2+} treated cells show reasonably good viability but other free divalent ions including Mn^{2+}, Co^{2+}, and Ni^{2+} show considerable toxicity on the cells even in a very low concentration (10 - 20 μg/ml). From these results, it is reasonable that our synthesized metal ferrite nanocrystals are stable and hardly release metal ions from the nanocrystals.
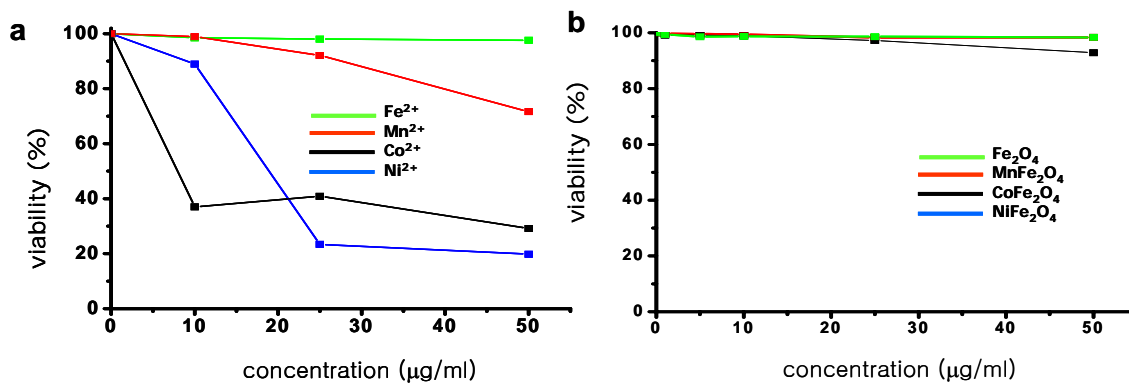
(Cheon J. *et. al. **unpublished data**.*)

Fig 4. Cytotoxicity profiles of free divalent metal ions (a) and metal ferrite nanocrystals (b) on macrophage.

4-3. *In vivo* stability of nanocrystals

We also examined the biodistribution of manganese ferrite nanocrystals in a live mouse (n=3) implanted with NIH3T6.7 at a proximal femur region. WSMIO-Herceptin conjugates were labelled with radio-active ^{111}In-DTPA compounds and then intravenously injected into the mouse. After 24 hrs, biodistribution of the conjugates was determined by using γ-counter analyses. In addition to being distributed in the tumor (3.4 %ID/g), our manganese ferrite nanocrystals were also distributed in the liver (12.8 %ID/g), spleen (8.7 %ID/g), and muscle (1.0 %ID/g) (%ID/g = injection-dose-percentages per gram) (Fig. 5). The blood half-life time of the WSMIO-Herceptin probes was determined to be ~194 min.
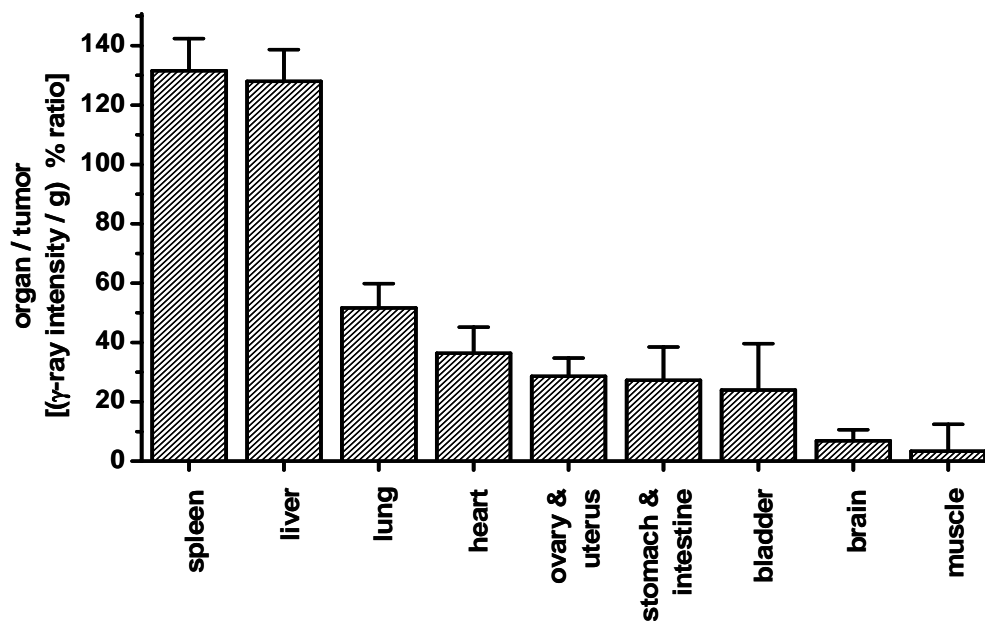
(Cheon J. *et. al.* **unpublished data**.)

Fig 5. Bio-distribution study of iron oxide nanocrystals

5. Pay-off

Inorganic nanocrystals which exhibit unique properties have the potential to be the key materials for next generation electronic devices, high density storage media, and biomedical diagnosis and treatment systems. Especially, magnetic nanocrystals can be used for magnetic sensing systems, magnetic target carriers for drug delivery, and magnetic information storages due to their special characteristics (small, enhanced magnetic properties, mobile, and highly water soluble). Therefore, the use of magnetic nanoparticles in biology offers next generation concept for the ultra fast real time detection and treatment of human disease.

Another important issue that requires attention before the utilization of any newly developed nanocrystals is an assessment of any deleterious biological properties that they may possess. From this project, the development of highly bio-compatible magnetic nanocrystals with low toxicity was possible and this accelerates the creation of next generation nanosystems for unique applications of biomedical technology.

6. Summary

In this project, *i*) we synthesized magnetic nanocrystals with various size, shape and composition. Through high temperature molecular precursor decomposition method we synthesized various nanocrystals such as metal, metal oxide, and core-shell type. With synthesized magnetic nanopaticles, *ii*) we performed the toxicity study including their composition toxic effect and surface capping molecule effect. Magnetic nanocrystals with various composition showed significantly reduced toxic effect compared to metal ions. In addition, surface modified nanocrystal with different capping molecules was also showed no harmful effect on cells. *iii*) We also studied the *in vivo* stability of nanocrystals through measuring their bio-distribution and blood half life using radio active isotope.

7. References

B. Xu *et al. J. Am. Chem. Soc.* **2003**, *125*, 15702.

D. R. Baselt, *et al. Biosensors & Bioelectronics* **1998**, *13*, 731.

J. Cheon, *et al. J. Am. Chem. Soc.* **2005**, *127*, 12387.

S. Goodwin *et al. J. Magn. Magn. Mater.* **1999**, *194*, 132.

W. J. Parak *et al. Nano Lett.* **2005**, *5*, 331.

J. Cheon *et al. Angewan. Chem.* **2006**, *45*, 3414.

J. Cheon *et. al. J. Phys. Chem. B* **2005**, *109*, 13119.

J. Cheon *et al. Chem. Commun.* **2006**, 1619.

J. Cheon *et al. J. Am. Chem. Soc.* **2005**, *127*, 5732.

J. Cheon *et al. J. Am. Chem. Soc.* **2005**, *127*, 9992.

8. Research outputs

8-1. Publications

1. Cheon, J. *et al.*
   "Langmuir Monolayers of Co Nanocrystals and Their Patterning by Microcontact Printing"
   The Journal of Physical Chemistry B 2005, *109*, 13119. [SCI I.F. = 3.834]

2. Cheon, J. *et al.*
   "Demonstration of a magnetic and catalytic Co@Pt nanocrystal as a dual-function nanoplatform"
   *Chem. Commun. **2006**, **1619**.* [SCI I.F. = 4.0]

8-2. Conferences

1. Cheon, J.
   "Magnetic Nanocrystals with Correlated Tunability for In Vivo MRI Cancer Diagnosis, Cell Trafficking, and Cytotoxicity"
   Gordon Research Conference on Clusters, Nanocrystals & Nanostructures, New London, CT, USA, Aug 3, 2005

2. Cheon, J.
   "Tailored Fabrication of Smart Nano-materials for Medical Sciences"
   11th Asian Chemical Congress, Korea Univ. Seoul, Korea, Aug 25, 2005

3. Cheon, J
   "Nanoscale Size Effect of Iron Oxide Nanocrystals and Their Biological Application for Cancer Diagnosis via Magnetic Resonance Imaging (MRI)"
   11th Asian Chemical Congress, Korea Univ. Seoul, Korea, Aug 25, 2005

4. Cheon, J.
   "Surface Modification of Magnetic Nanocrystals for Efficient Intracellular Labeling and In Vivo MR Trafficking"
   11th Asian Chemical Congress, Korea Univ. Seoul, Korea, Aug 25, 2005

5. Cheon, J.

"Tailored Fabrication of Smart Nano-materials for Bio-Medical Diagnosis"

Materials Research Society Meeting, MRS, Boston, MA, U.S.A., Nov. 28, 2005

6. Cheon, J.

"In situ One-Pot Synthesis of 1-Dimentional Transition Metal Oxide Nanocrystals"

Materials Research Society Meeting, MRS, San Francisco, CA, U.S.A., Apr. 20, 2006

9. Financial Reports

I. Planned Expenditure (Nov. 1, 2004~ Oct. 31, 2005)	II. EXPENDITURES
SALARIES A. SENIOR PERSONNEL $ 9,000 B. OTHER PERSONNEL $ 1,000	SALARIES A. SENIOR PERSONNEL: $ 9,000 Jinwoo Cheon : $ 3,000 * 3 month = $ 9,000 B. OTHER PERSONNEL $ 1,000 Jung-Wook Seo: $ 1,000 * 0.20 * 5 = $ 1,000

D. EQUIPMENT $ 0
 	
E. TRAVEL $ 5,500
 	
F. TUITION REF 2.12.13 $ 0
	D. EQUIPMENT $ 0
	
	E. TRAVEL $ 5,500
	
	  Jinwoo Cheon
	
	   Taejeon (ETRI), research meeting $ 300X5 =$1500
	
	  Seung-won Park
	
	   Taejeon (KBSI), SQUID analysis $80X6 = $480
	
	  Jung-tack Jang
	
	   Taejeon (KBSI), SQUID analysis $80X5 = $400
	
	  Jung-wook Seo
	
	   Taejeon (KRICT), GC analysis $80
	
	  Prepaid expenditures
	
	  Jin-sil Choi
	
	   Taejeon (KBSI), TEM analysis $40X28 = $1120
	
	  Jinwoo Cheon
	
	   Jeju, The 13th Korea-Japan Joint Symposium on Organometallic and Coordination Chemistry
	
	   Airfare $500 + Travel cost $500 = $1000
	
	  Busan, Korea-Japan Joint Symposium on Chemistry of Transition Metal Compounds
	
	   Airfare $420 + Travel Cost $500 = $920
	
	F. TUITION REF 2.12.13 $ 0

G. OTHER DIRECT COSTS $ 3,200	G. OTHER DIRECT COSTS $ 3,200
1. SUPPLIES/MATERIALS $ 2,200	1. SUPPLIES/MATERIALS $ 2,200
	* See the detailed materials sheet.
2. Utility $ 1,000	2. Utility $1,000
	telephone fee $75 * 12 = $900
	copies $100
J. TOTAL DIRECT EXPENSES AND FACILITIES AND ADMINISTRATION EXPENSES Overhead $ 6,300	J. TOTAL DIRECT EXPENSES AND FACILITIES AND ADMINISTRATION EXPENSES Overhead $ 6,300
Total: $25,000	Total: $25,000

* Detailed materials sheet

Item	Unit price ($)	Amount	Total ($)
Iron pentacarbonyl (Strem 26-2800, 250 g)	30.00	10	300.00
Oleic acid (Sigma O1383, 25 g)	150.00	2	300.00
Sephadex G-25 (Sigma S5772, 25g)	180.00	1	180.00
TBE buffer (Sigma T4415, 10x, 20 L)	230.00	2	460.00
M_2C_2H	165.00	3	495.00
1,2-Hexadecanediol, Tech (Aldrich 213748, 50g)	132.50	2	165.00
Iron(III) acetylacetonate (Aldrich 517003, 50g)	100. 0	3	300.00
Total			$ 2,200

* Appendices

Demonstration of a magnetic and catalytic Co@Pt nanoparticle as a dual-function nanoplatform†

Chul-Ho Jun,*[a] Young Jun Park,[a] Ye-Rim Yeon,[a] Joon-rak Choi,[b] Woo-ram Lee,[b] Seung-jin Ko[b] and Jinwoo Cheon*[b]

Co@Pt nanoparticles as a bifunctional nanoplatform system for the hydrogenation of various unsaturated organic molecules under mild conditions and also for magnetic separation and recycling are demonstrated.

Nanoparticles (NPs) with extremely large surface areas can possess various functions, such as catalytic, magnetic, electronic and optical properties. In particular, with the emerging interest in developing versatile NPs for nanoplatform technologies, NPs exhibiting more than two functions are highly desirable for simultaneous and efficient technological applications. NPs with a core–shell structure are one of the promising candidates for integrating multiple functionalities into a single NP system.[1] Such core–shell nanostructures have been shown to be very useful for enhancing or modifying the properties of NPs, such as the surface plasmonic effect observed in the SiO_2@Au nanoshell and bimetallic nanocatalysts, for example the Co–Rh system.[2] Although the large surface area of NP-based catalysts is the key component of their catalytic activity,[3–5] as the size of the particle decreases to a nanometer scale, its separation step becomes harder and particle agglomeration during the reaction or separation process becomes a troublesome issue.[5] To circumvent such problems in nanocatalyst synthesis, various possibilities have been examined. For example, catalytic Pt NPs can be stabilized by large organic polymers or encapsulated within porous materials such as zeolites.[6] Herein, we present the core–shell Co@Pt NP and demonstrate both the catalytic activity (hydrogenation) of its Pt shell and the superparamagnetism of its Co core, which allows for the convenient separation and recycling of the nanocatalyst (Fig. 1). To our knowledge, our study is one of the first demonstrations of magnetically recovering heterogeneous catalytic NPs,[7] although examples of homogenous organometallic catalysts ligated with magnetic NPs have been reported previously.[8]

Our core–shell-type platinum NP catalyst (**1**) can provide advantages over single Pt component-based systems: Firstly, it is "atomically economical" because precious Pt metal can be conserved by replacing the interior of the NPs with other,

[a]Department of Chemistry, Yonsei University, Seoul 120-749, Korea. E-mail: junch@yonsei.ac.kr; Fax: (+82) 2 3147 2644; Tel: (+82) 2 2123 2644
[b]Department of Chemistry and Nanomedical National Core Research Center, Yonsei University, Seoul 120-749, Korea. E-mail: jcheon@yonsei.ac.kr; Fax: (+82) 2 364 7050; Tel: (+82) 2 2123 5631
† Electronic Supplementary Information (ESI) available: Catalytic procedures, GC-MS data and elemental analysis. See DOI: 10.1039/b600147e
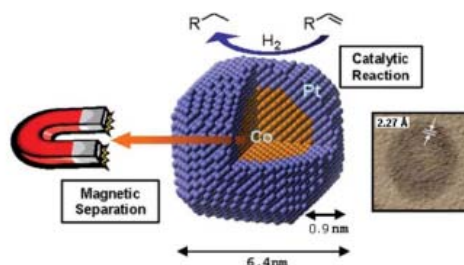

Fig. 1 The dual functionality of Co@Pt core–shell NPs. Insert: The HRTEM image of a single NP. 2.27 Å represents the lattice constant of the Pt shell.

inexpensive core metals.[9] Secondly, the additional functionality of the magnetic cobalt core[10] plays a critical role in the separation and recycling of the catalyst.

The core–shell type-cobalt–platinum NPs were prepared by a redox transmetalation reaction between $Pt(hfac)_2$ and cobalt NPs.[11] The platinum forms a shell around the cobalt core and the shell surface is stabilized by dodecyl isocyanide capping molecules (Fig. 1). After the formation of the core–shell structure, the NP retains its magnetic properties, with a blocking temperature (T_B) of 15 K and a coercivity of 660 Oe at 5 K, indicating single domain superparamagnetism at room temperature. The particle size averages 6.4 nm with a cobalt core diameter of 4.6 nm; its overall stoichiometry being $Co_{0.45}Pt_{0.55}$. According to elemental analysis and high resolution transmission electron microscopy (HRTEM) data, the thickness of the Pt layer is about ~0.9 nm, which corresponds to ~4 layers of Pt.[11] A particle size of 6.4 nm was chosen because it gives a high colloidal stability while keeping a high surface area of Pt and strong magnetism. It is desirable to minimize the use of Pt as much as possible for economic reasons. In contrast, if the particle becomes too small (e.g. < 5 nm), the cobalt core also becomes smaller and does not have a strong enough magnetism for magnetic recycling processes. In short, our rationale for selecting the NP composition and size was to have **1**: a high surface area for the Pt shell with minimum use of it, 2: retention of high magnetism for recycling purposes and 3: high colloidal stability for the dispersion of the nanocatalysts into the reaction solution. Since our core–shell cobalt–platinum NPs are well dispersed in a typical organic medium, we investigated the catalytic activity and recyclability of **1** towards hydrogenation, using 1-decene as a model substrate (Table 1).

Table 2 Hydrogenation of various substrates[a]

Entry	Substrate	Product	Time/h	Conversion (%)[b]
1	1-Decene	n-Decane	4	100
2	1,5,9-Decatriene	n-Decane	4	100
3	Cyclododecene	Cyclododecane	4	100
4	Styrene	Ethylbenzene	6	100
5	1-Octyne	n-Octane	8	100
6	4-Octyne	n-Octane	10	100
7	3-Phenylpropyne	Propylbenzene	4	100
8	1-Phenylpropyne	Propylbenzene	4	100
9	Diphenylacetylene	1,2-Diphenylethane	14	17
10	Benzaldehyde	Benzylalcohol	16	100
11	Cyclohexanone	—	12	0
12	Cinnamaldehyde[c]	Hydrocinnamylalcohol	10	100[c]
13	2-Cyclohexenone	Cyclohexanone	7	100
14	Nitrobenzene	Aniline	4	100
15	2-Bromonitrobenzene	2-Bromoaniline	16	100[d]

[a] Reaction conditions: Substrate 0.25 mmol, substrate/Pt atom = 50 (2 mol%), toluene 0.1 mL, 1 atm H_2 (using toy balloon), room temperature. [b] Determined by GC and GC–MS. [c] Mixture of partially and fully hydrogenated products. [d] Containing less than 1% of debrominated product.

capabilities. This kind of bifunctional core–shell NP may provide useful applications in various types of transition metal-based catalytic reaction.

Notes and references

‡ It is noteworthy that we have not observed any hydrogenation product from the capping molecule in any of these catalytic reactions.

1 (a) S. Sun, C. B. Murray, D. Weller, L. Folks and A. Moser, *Science*, 2000, **287**, 1989; (b) V. Klimov, A. A. Mikhailovsky, S. Xu, A. Malko, J. A. Hollingsworth, C. A. Leatherdale, H.-J. Eisler and M. G. Bawendi, *Science*, 2000, **290**, 314; (c) X. Zhong, M. Han, Z. Dong, T. J. White and W. J. Knoll, *J. Am. Chem. Soc.*, 2003, **125**, 8589; (d) X. Peng, M. C. Schlamp, A. V. Kadavanich and A. P. Alivisatos, *J. Am. Chem. Soc.*, 1997, **119**, 7019.

2 (a) K. H. Park and Y. K. Chung, *Adv. Synth. Catal.*, 2005, **347**, 854; (b) C. Radloff and N. J. Halas, *Nano Lett.*, 2004, **4**, 1323; (c) T. Pham, J. B. Jackson, N. J. Halas and T. R. Lee, *Langmuir*, 2002, **18**, 4915.

3 (a) L. N. Lewis, *Chem. Rev.*, 1993, **93**, 2693; (b) A. P. Alivisatos, *Science*, 1996, **271**, 933; (c) A. Henglein, *Chem. Rev.*, 1989, **89**, 1861.

4 (a) C.-W. Chen, T. Serizawa and M. Akashi, *Chem. Mater.*, 1999, **11**, 1381; (b) H. Weller, *Angew. Chem., Int. Ed. Engl.*, 1993, **32**, 41; (c) A. Henglein, *J. Phys. Chem.*, 1993, **97**, 5457.

5 (a) J. A. Widegren and R. G. Finke, *J. Mol. Catal. A: Chem.*, 2003, **191**, 187; (b) A. Roucoux, J. Schulz and H. Patin, *Chem. Rev.*, 2002, **102**, 3757.

6 (a) J. W. Yoo, D. Hathcock and M. A. El-Sayed, *J. Phys. Chem. A*, 2002, **106**, 2049; (b) P. Concepción, A. Corma, J. Silvestre-Albero, V. Franco and J. Y. Chane-Ching, *J. Am. Chem. Soc.*, 2004, **126**, 5523; (c) M. Arai, Y. Takada and Y. Nishiyama, *J. Phys. Chem. B*, 1998, **102**, 1968; (d) M. Zhao and R. M. Crooks, *Angew. Chem., Int. Ed.*, 1999, **38**, 364; (e) S. Mandal, D. Roy, R. V. Chaudhari and M. Sastry, *Chem. Mater.*, 2004, **16**, 3714; (f) N. Guillon, Q. Gao, P. M. Forster, J.-S. Chang, M. Nogues, S.-E. Park, G. Ferey and A. K. Cheetham, *Angew. Chem., Int. Ed.*, 2001, **40**, 2831.

7 Z. Chang, C.-X. Guo, F. Li, X. Duan and M.-L. Zhang, *Acta Chim. Sin.*, 2002, **60**, 298.

8 (a) T.-J. Yoon, W. Lee, Y.-S. Oh and J.-K. Lee, *New J. Chem.*, 2003, **27**, 227; (b) P. D. Stevens, J. Fan, H. M. R. Gardimalla, M. Yen and Y. Gao, *Org. Lett.*, 2005, **7**, 2085; (c) A. Hu, G. T. Yee and W. Lin, *J. Am. Chem. Soc.*, 2005, **127**, 12486; (d) S. C. Tsang, V. Caps, I. Paraskevas, D. Chadwick and D. Thompsett, *Angew. Chem., Int. Ed.*, 2004, **43**, 5645.

9 S. U. Son, Y. Jang, J. Park, H. B. Na, H. M. Park, H. J. Yun, J. Lee and T. Hyeon, *J. Am. Chem. Soc.*, 2004, **126**, 5026.

10 (a) H. Srikanth, E. E. Carpenter, L. Spinu, J. Wiggins, W. Zhou and C. O'Connor, *Mater. Sci. Eng., A*, 2001, **304**, 901; (b) W. L. Zhou, E. E. Carpenter, J. Lin, A. Kumbhar, J. Sims and C. J. O'Connor, *Eur. Phys. J. D*, 2001, **16**, 289.

11 For the preparation of 1, its magnetic properties and full characterization data, see: J.-I. Park and J. Cheon, *J. Am. Chem. Soc.*, 2001, **123**, 5743.

12 In terms of the recoverability, it is noteworthy that the turnover frequencies (TOF) of 1 were constant (2 h^{-1}) during the seven cycles. However, in the control experiment using Pt/C (2 mol%) as a hydrogenation catalyst, the TOFs of Pt/C rapidly reached half the value (4.16 h^{-1}) of the initial TOF (8 h^{-1}) at the fifth cycle: 100% (1st cycle), 100% (2nd cycle), 76% (3rd cycle), 67% (4th cycle), 52% (5th cycle). Although the TOFs of Pt/C are apparently higher than those of 1, it seems to be difficult to compare the catalytic activity of 1 with that of Pt/C directly, because there is a significant difference in their nature: the existence or non-existence of the capping ligand in each system. For a similar discussion, see: (a) C. A. Stowell and B. A. Korgel, *Nano Lett.*, 2005, **5**, 1203. Special issue on recoverable catalysts and reagents; (b) J. A. Gladysz, *Chem. Rev.*, 2002, **102**, 3215.

13 S. Ichikawa, M. Tada, Y. Iwasawa and T. Ikariya, *Chem. Commun.*, 2005, 924.

20

Langmuir Monolayers of Co Nanoparticles and Their Patterning by Microcontact Printing

Jong-Il Park,[†] Woo-Ram Lee,[‡] Sung-Soo Bae,[†] Youn Joong Kim,[§] Kyung-Hwa Yoo,[‡] Jinwoo Cheon,*,[‡] and Sehun Kim*,[†]

Department of Chemistry, Korea Advanced Institute of Science and Technology, Daejeon 305-701, Korea, Departments of Chemistry and Physics, Yonsei University, Seoul 120-749, Korea, and Division of Nano-Material and Environmental Science, Korea Basic Science Institute, Daejeon 305-333, Korea

Received: December 13, 2004; In Final Form: April 18, 2005

In this paper, we describe an easy and reliable method for the production of patterned monolayers of Co nanoparticles. A two-dimensional monolayer of Co nanoparticles is fabricated by spreading a nanoparticle solution over an air−water interface and then transferring it to a hydrophobic substrate by using the Langmuir−Blodgett (LB) method. Transmission electron microscopy (TEM) was used to show that, with increasing surface pressure, the Co nanoparticles become well-organized into a Langmuir monolayer with a hexagonal close-packed structure. By controlling the pH of the subphase, it was found that a monolayer of Co nanoparticles with long-range order could be obtained. Further, by transferring the Langmuir monolayer onto a poly-(dimethoxysilane) (PDMS) mold, the selective micropatterning of the Co nanoparticles could be achieved on a patterned electronic circuit. The electronic transport properties of the Co nanoparticles showed the ohmic *I*−*V* curve.

Introduction

Convenient and effective organization of nanomaterials (molecules, polymers, and nanoparticles) into one-, two-, and three-dimensional (1-D, 2-D, and 3-D) structures is the key to the realization of nanodevices.[1−8] The most common method of constructing 2- and 3-D nanoparticle structures involves synthesizing the nanoparticles in solution by chemical methods and then attaching them to various substrates using suitable interactions such as van der Waals forces and electrostatic or covalent bonds.[9−11] In the case of Au nanoparticles, 1-D chains and wires have been produced along nanofibrils derived from the self-assembly of DNA and synthesized peptides.[9,10,12] Three-dimensinal crystal structures have been formed by a self-assembly process with a ligand exchange reaction.[13] During the self-assembly process, 2-D monolayers are produced as a result of interparticle interactions. To more effectively produce 2-D monolayers of nanoparticles on solid substrates, many research-ers have tried using various techniques, such as layer by layer (LbL) deposition, the Langmuir−Blodgett method (LB), and the spin-coating method.[14−16] The LB technique is the most promising method for producing well-organized 2-D monolayers of surfactants, polymers, and nanoparticles, because it provides fine control of the thickness and homogeneity of the monolayer and of multilayers. For example, Heath et al., Markovich et al., and Xi et al. have reported the fabrication of LB films of Ag, Fe₃O₄, and Fe₂O₃ nanoparticles in the presence of various capping molecules such as fatty acids and alkanethiols.[16−18] Furthermore, the formation of 2-D patterned monolayers of Au, Fe₂O₃, and Pt@Fe₂O₃ nanoparticles by using a combination of LB with microcontact printing (μ-CP) has been reported.[19−22]

However, highly ordered LB films and 2-D patterns of Co nanoparticles have not yet been reported because of difficulties in the synthesis of monodisperse Co nanoparticles.

In this paper, we describe a method for the systematic and comprehensive fabrication of 2-D monolayers of Co nanopar-ticles via the LB technique and of 2-D patterned monolayers on various substrates, such as silicon wafers, using the micro-contact printing method.

Experimental Section

Materials. Octadecyltrichlorosilane (OD-TCS) and sodium bis(2-ethylhexyl) sulfosuccinate (NaAOT) were purchased from Aldrich Co. Tetradecanoic acid and all solvents were purchased from Junsei Co. Dicobalt octacarbonyl was purchased from Strem Inc. Deionized (DI) water (18 MΩ·cm) was obtained using a Millipore four-bowl purification system. PDMS elas-tomer (Sylgard 184) was obtained from Dow Corning.

Preparation of Co Nanoparticles. Co nanoparticles were prepared using the thermolysis of Co₂(CO)₈ in a refluxing toluene solution containing tetradecanoic acid and NaAOT as stabilizer.[23] The Co nanoparticles solution was filtered through a 0.45 μm nylon membrane filter to remove aggregated nanoparticles and residual organic impurities.

Substrate Preparation. The Si(111) surface was cleaned by dipping it in piranha solution (H₂SO₄:H₂O₂ = 7:3) at 90 °C for 1 h followed by washing with deionized water. After cleaning, the sample was sonicated in basic hydroxide solution (H₂O: H₂O₂:NH₃ = 5:1:1) for 30 min, then sonicated in acidic peroxide solution (H₂O:H₂O₂:HCl = 6:1:1) for 30 min followed by washing with deionized water, and kept in an oven at 120 °C for 10 min. The slide glasses, oxidized Si(111) wafers, and mica substrates were also cleaned by sonication in 2-propanol.

The OD-terminated surface was produced by immersion in a toluene solution (20 mL) containing OD-TCS (0.1 mL) at room temperature (RT) for 10 min. After the reaction, each

* To whom correspondence should be addressed. (S.K.) Phone: (+82) 42-869-2831. Fax: (+82) 42-869-2810. E-mail: sehun-kim@kaist.ac.kr. (J.C.) Phone: (+82) 2-2123-5631. Fax: (+82) 2-364-7050. E-mail: jcheon@yonsei.ac.kr.
  † Korea Advanced Institute of Science and Technology.
  ‡ Yonsei University.
  § Korea Basic Science Institute.

Langmuir Monolayers of Co Nanoparticles

J. Phys. Chem. B, Vol. 109, No. 27, 2005 **13123**

current through the monolayer of nanoparticles between the two electrodes. The patterned samples are electrically insulating because of the long-chain organic capping groups and the surface oxide layer.[24] After annealing the substrate for 1 h under reducing conditions (300 °C, 5% H₂), ohmic transport was observed in this pattern at room temperature instead of the Coulomb blockade, as shown in Figure 6E.[24] Multichannel tunneling through the hexagonally packed nanoparticles is a major contribution to the electron transport, contributing more to the ohmic conductivity than single particle transport.[25,26] Room-temperature resistance is about 120 kΩ, which is similar to the value for annealed Co nanoparticles obtained by Black et al.[6] Low-temperature transport measurements were not carried out in this study, but the resulting transport is expected to be similar to Black's results.

If a suitable PDMS pattern and gold electrode substrate with a nanoscale pattern are prepared, the LB—μCP method could be used in the future fabrication of nanodevices, such as single-electron transistors with a high-density array.

Conclusion

In summary, the forced assembly of Co nanoparticles on an air—water interface can be used to produce a wide range of ordered Co nanoparticle films that under optimum conditions can be easily transferred to hydrophobic substrates. The hexagonal close-packing structures of the LB films were controlled by variation of the particle concentration, the pH of the subphase, the barrier rate, and the dipping rate. Further, patterning of the Co nanoparticles was achieved by stamping a Langmuir film coated onto a PDMS stamp; these patterns were characterized by optical microscopy and FE-SEM. Furthermore, we suggest that future nanodevices can be manufactured by selectively imprinting Langmuir monolayers of nanoparticles onto patterned gold electrodes.

Supporting Information Available: Two figures, showing (S1) X-ray photoelectron spectra and X-ray absorption spectra and (S2) TEM and FE-SEM images (PDF). This material is available free of charge via the Internet at http://pubs.acs.org.

References and Notes

(1) Schmid, G. *Nanoparticles: From Theory to Application*; Wiley-VCH: Weinheim, Germany, 2004; p 1.

(2) Pole, C. P.; Owens, F. J. *Introduction to Nanotechnology*; Wiley-Interscience: New Jersey, 2003; p 1.

(3) Klabunde, K. J. *Nanoscale Materials in Chemistry*; Wiley-Interscience: New York, 2001; p 1.

(4) Pileni, M. P. *Metal Nanoparticles: Synthesis, Characterization, and Applications*; Dekker: New York, 2001; p 1.

(5) Sun, S. H.; Murray, C. B.; Weller, D.; Folks, L.; Moser, A. *Science* **2000**, *287*, 1989.

(6) Black, C. T.; Murray, C. B.; Sandstrom, R. L.; Sun, S. H. *Science* **2000**, *290*, 1131.

(7) Petit, C.; Taleb, A.; Pileni, M. P. *J. Phys. Chem. B* **1999**, *103*, 1805.

(8) Boal, A. K.; Ilhan, F.; DeRouchey, J. E.; Thurn-Albrecht, T.; Russell, T. P.; Rotello, V. M. *Nature* **2000**, *404*, 746.

(9) Maeda, Y.; Tabata, H.; Kawai, T. *Appl. Phys. Lett.* **2001**, *79*, 1181.

(10) Fu, X. Y.; Wang, Y.; Huang, L. X.; Sha, Y. L.; Gui, L. L.; Lai, L. H.; Tang, Y. Q. *Adv. Mater.* **2003**, *15*, 902.

(11) Bae, S. S.; Lim, D. K.; Park, J. I.; Lee, W. R.; Cheon, J.; Kim, S. *J. Phys. Chem. B* **2004**, *108*, 2575.

(12) Loweth, C. J.; Caldwell, W. B.; Peng, X. G.; Alivisatos, A. P.; Schultz, P. G. *Angew. Chem., Int. Ed.* **1999**, *38*, 1808.

(13) Baraton, M.-I. *Synthesis, Functionalization and Surface Treatment of Nanoparticles*; American Scientific Publishers: Stevenson Ranch, CA, 2003; p 1.

(14) Basu, J. K.; Sanyal, M. K. *Phys. Rep.* **2002**, *363*, 1.

(15) Hong, Y. K.; Kim, H.; Lee, G.; Kim, W.; Park, J. I.; Cheon, J.; Koo, J. Y. *Appl. Phys. Lett.* **2002**, *80*, 844.

(16) Heath, J. R.; Knobler, C. M.; Leff, D. V. *J. Phys. Chem. B* **1997**, *101*, 189.

(17) Fried, T.; Shemer, G.; Markovich, G. *Adv. Mater.* **2001**, *13*, 1158.

(18) Huo, H.; Li, W.; Cui, H.; Xi, S.; Wang, J.; Zhao, B.; Shen, Y.; Lu, Z. *Chem. Mater.* **2000**, *13*, 790.

(19) Santhanam, V.; Liu, J.; Agarwal, R.; Andres, R. P. *Langmuir* **2003**, *19*, 7881.

(20) Santhanam, V.; Andres, R. P. *Nano Lett.* **2004**, *4*, 41.

(21) Guo, Q.; Teng, X.; Rahman, S.; Yang, H. *J. Am. Chem. Soc.* **2003**, *125*, 630.

(22) Guo, Q.; Teng, X.; Yang, H. *Adv. Mater.* **2004**, *16*, 1337.

(23) Park, J. I.; Kang, N. J.; Jun, Y. W.; Oh, S. J.; Ri, H. C.; Cheon, J. *ChemPhysChem* **2002**, *3*, 543.

(24) As-prepared Co nanoparticles are oxidized during LB filming procedure in basic solution and ambient condition but easily reduced by annealing at 300 °C under H₂ gas. (See Supporting Information.)

(25) Petit, C.; Cren, T.; Roditchev, D.; Sacks, W.; Klein, J.; Pileni, M. P. *Adv. Mater.* **1999**, *11*, 1198.

(26) We have compared the SEM images before and after reduction at 300 °C under H₂. After the reducing process, the interparticle distance was shortened and the oxidized CoO layer and stabilizer of Co nanoparticles were removed. The shortened interparticle distance and reduction of the oxidized state are attributed to the conductance of Co nanoparticle films (Figure S2 in Supporting Information).